Evaluation of antibacterial effect on *Escherichia coli* PTCC 1395 of TiO_2 nanoparticles synthesized via sol-gel method

ALI ABDOLAHZADEH ZIABARI[a,*], SAJIHE BAHREKAZEMI[b]
[a]*Department of Physics, Faculty of Science, Lahijan Branch, Islamic Azad University, P.O. Box1616 , Lahijan, Iran*
[b]*Department of Microbiology, Faculty of Science, Lahijan Branch, Islamic Azad University, Lahijan, Iran*

Titanium dioxide (TiO_2) nanoparticles were synthesized by sol-gel method and their physico-chemical properties were characterized by scanning electron microscopy (SEM), X-ray diffraction (XRD), and Fourier transform infrared spectroscopy (FTIR). Using the well-known Scherrer formula, the size of nanoparticles was estimated. This was 28.70, 31.05 and 32.94 nm for 0.1, 0.3 and 1 molar nanoparticle concentrations, respectively. The TiO_2 nanoparticles prepared at 0.1 M had only anatase phase, but at 0.3 and 1 M both anatase and rutile phases were observed. The photocatalytic property of TiO_2 nanoparticles was investigated by inactivation of *Escherichia coli* PTCC 1395 under irradiation by a UV-B lamp. The sharp peaks in FTIR spectrum indicated the purity of TiO_2 nanoparticles. The TiO_2 nanoparticles have a significant antibacterial effect on *Escherichia coli* PTCC 1395 at concentration of 1mg/mL. Increasing the molarity from 0.1 to 1 M, decreased the viable cell concentration of *Escherichia coli* PTCC 1395 from 88.89 % to 8.33 % after 3 hours.

(Received October 2, 2013; accepted March 13, 2014)

Keywords: Escherichia coli PTCC 1395, Titanium dioxide, nanoparticle, Sol-gel, Photocatalytic

1. Introduction

Titanium dioxide (TiO_2) plays an important role in our environmental purification due to its no toxicity, photocatalytic activity, photo induced super-hydrophilicity and antifogging effects [1]. TiO_2 photocatalysis is a technique for decontamination and purification of air and wastewater [2-6] being also applied to inactivate bacteria, viruses, and cancer cells [7-10]. TiO_2 contains three crystalline phases including anatase, rutile and brookite. Amongst these phases, rutile is more stable and the other two converts to rutile phase as a result of heating. Investigations showed that activity of catalytic anatase is stronger than that of other phases. The antibacterial properties of TiO_2 nanoparticles are attributed to the high redox potential of the surface species formed by photo-excitation affording non-selective oxidative attack of bacteria [11]. Photocatalytic inactivation of bacteria leads to formation of reactive oxygen species (ROS), such as hydroxyl radical, hydrogen peroxide, superoxide radical, etc. [9,10, 12-22]. The type and the source of TiO_2 has a large role during bacterialinactivation due to the rate of ROS formation, the particle size, the isoelectric point, crystalline phase, Brunauer, Emmet and Teller (BET) specific surface area, aggregate size in suspension solution and to other factors [11]. On the other hand, depending on experimental conditions, TiO_2 photocatalytic process may destroy some microorganisms [23-33]. In general, the biological agents of the microorganisms such as microbial species, growth phase, initial cell density, etc. are also important and the photocatalytic disinfection process may vary depending on the light intensity, the UV wavelengths and other experimental conditions. TiO_2 nanoparticles can be synthesized by a variety of routes including sol-gel method, hydrothermal method, solvothermal process, plasma evaporation, ball milling, etc. [31, 34]. In this work, three different molarity of TiO_2 nanopowder were synthesized by the low temperature sol-gel method and their antibacterial action against *Escherichia coli* PTCC 1395 was studied.

2. Experimental

2.1. Materials and methods

First of all, the necessary liquid medium containing crystalline TiO_2 nanoparticles were prepared using sol-gel method. 1, 3 and 10 mL tetra-n-butyl orthotitanate (Merck, 99 %) was slowly added dropwise into 30 mL ethanol (Merck, 99.8 %) under vigorous stirring at room temperature. Afterward, 0.75 mL acetylacetone was introduced to the above prepared mixture. Then, 0.2 mL of HCl solution was added. Finally, a transparent yellowish mixture was formed. The prepared solution was dried at 60 °C for 24-48 hours, leading to an amorphous gel. The extracted powder was then annealed at 700 °C for 2 hours leading to white crystalline TiO_2 nanoparticles.

2.2. Characterizing TiO_2 nanoparticles

The structure and morphology of the resulting particles were characterized by X-ray diffraction (XRD) at room temperature, in the $4° < 2\theta < 94°$ range (Bruker D_8 Advance, CuK_α radiation) and Scanning Electron Microscopy (SEM) by a VEGAII TESCAN instrument. FTIR studies in cell with CaF_2 windows, where samples were located, were carried out in a FTIR spectrophotometer model RS/1 from UNICAM. Water reference spectrum was always subtracted from every spectrum in the region between 1,800 and 1,000 cm^{-1}.

2.3. Biological experimental procedure

One standard bacterial strain was tested: *Escherichia coli* (PTCC 1395). One colony of this culture was inoculated into nutrient broth and then incubated under aerobic conditions at 37 °C for 15-17 h. During the steady state growth phase, bacterial cells were harvested by centrifugation at 10,000 rpm for 15 min. The bacterial pellets were subsequently washed twice with 10 mL of sterile phosphate buffered saline (PBS) at pH = 7.2. The final pellets were resuspended with PBS in sterile tubes and standardized using apparatus to 0.5 Mc Farland which corresponds to the cell density of 1.5×10^8 colony forming units (CFU) per mL. The disinfection process was accomplished at the following parameters: initial cell density about 1.5×10^8 CFU/mL; concentration of TiO_2 nanoparticles of 1mg/mL; UV-B lamp (Philips) with the major fraction of irradiation occurring at 280-315 nm, situated sidewise at a distance of 45 cm to the reaction vessels for 3 hours. TiO_2 nanoparticles with a concentration of 1mg/mL were added into cell with a density of about 1.5×10^8 CFU/mL and then incubated at 37 °C for 3 hours. Afterward, 1mL from any experimental tubes was withdrawn and serial dilutions were prepared before plating. The number of viable cells was determined by pour plate method as following: 100 µL from any dilution were prepared in duplicate on nutrient agar, poured in Petri dishes with agar depth of 5 mm. After overnight incubation at 37 °C, the colonies on the plates were counted and results were calculated to 1 mL.

3. The results and conclusion

Fig. 1 presents the XRD patterns (a, b, c) of TiO_2 the obtained by sol-gel method. The mean size of the ordered anatase TiO_2 nanoparticles has been estimated from full width at half maximum (FWHM) and Debye-Scherrer formula as follows:

$$D = \frac{0.89\lambda}{\beta \cos\theta} \quad (1)$$

where, 0.89 is the shape factor, λ is the X-ray wavelength, β is the line broadening at half the maximum intensity (FWHM) in radians, and θ is the Bragg angle. Using different amount of the starting materials, the obtained crystallite sizes are different. The average crystallite sizes of the obtained TiO_2 are about: 28.70, 31.05, and 32.94 nm, respectively. TiO_2 can have three types of crystal structures: anatase (A) type, rutile (R) type, and brookite (B) type. Among these, anatase type is known to have a higher photocatalytic activity due to the difference in the position of the conduction bands [35]. The prepared TiO_2 nanoparticles at 0.1 molar concentration have only anatase phase which has intensity at peaks: (101), (103), (004), (112), (200), (105), (211), (118), (116), and (220) (Fig.1-a), but at 0.3 and 1 M both anatase and rutile phases are observed having intensity at peaks: (101), (110), (101), (004), (111), (210), (200), (211), (002), (310), and (310) (Fig. 1-b,c). Fig. 2 shows the SEM images of TiO_2 nanoparticles. To take these images, firstly the nanopowder was prepared in the form of pellet. This comparative picture shows some aggregates that contains nanocrystallites. Fig. 2-c shows the SEM image of *Escherichia coli* after being damaged by the nanoparticles. Comparing with Fig. 2-a and Fig. 2-b, one indicates that TiO_2 nanoparticles have effectively deteriorated the bacteria. The anatase type TiO_2 absorbs photons in the UV range of the solar spectrum exciting the valence electrons and generating the Electron-Hole Pairs (EHPs). These EHPs then recombine and become adsorbed on or near the surface of TiO_2. These excited electrons and holes have high redox activities and hence react with water and oxygen yielding ROS, such as super oxide anions (O_2^{-}) and hydroxyl radicals ($^{\bullet}OH$). TiO_2 photocatalysts on irradiation with light of suitable wavelength causes the formation of ROS initiating a cascade of redox reactions which can mineralize a variety of organic compounds [36, 37].

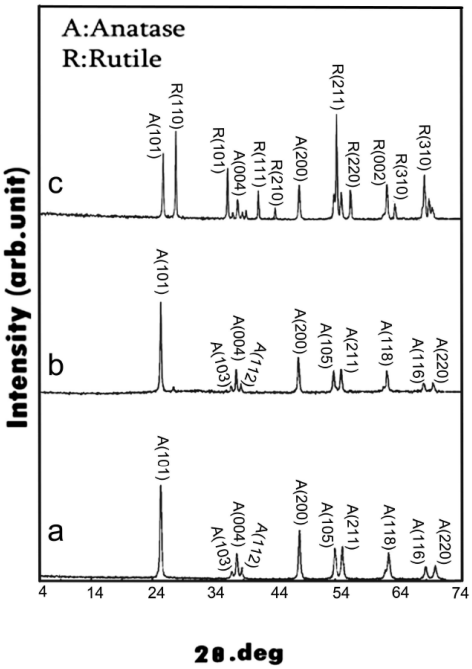

Fig. 1. The XRD patterns of (a) 0.1 M, (b) 0.3 M and (c) 1 M TiO_2 nanoparticles.

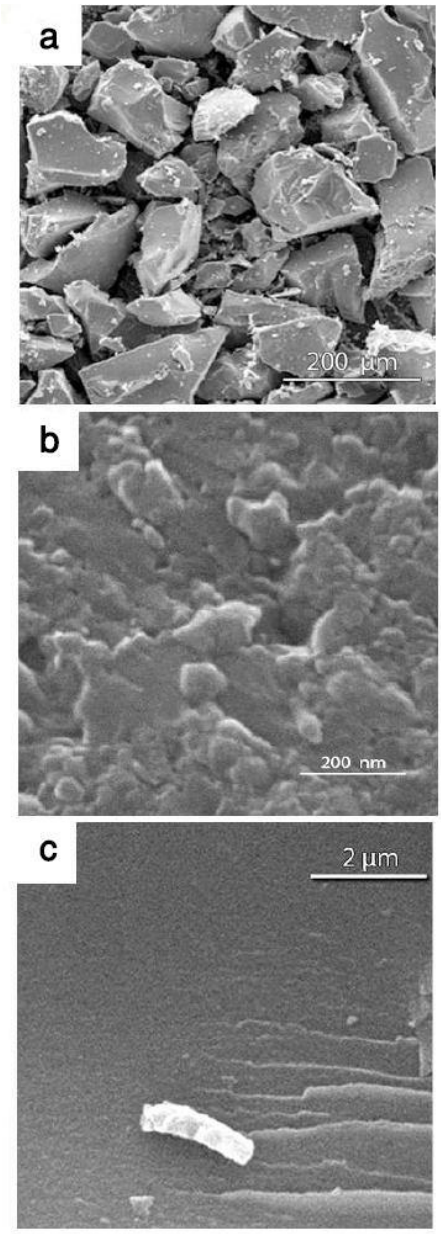

Fig. 2. SEM micrograph of (a) 1 M (200 µm), (b) 1 M (200 nm) concentration of TiO_2 nanoparticles and (c) the micrograph of Escherichia coli after being damaged by the nanoparticles of TiO_2.

Fourier transform infrared (FTIR) spectroscopy is the most useful for identifying types of chemical bonds (functional groups). The wavelength of light absorbed is characteristic of the chemical bond. The FTIR spectrum of the synthesized TiO_2 nanoparticles was recorded in the range, 400-4,000 cm^{-1}, (Fig. 3). The large broad bands at 3,200-4,000 cm^{-1} are due to the O-H stretching. The sharp bands situated at 1,600 cm^{-1} can be assigned to the stretched bending of H-O-H due to H_2O on the nanoparticles surface. Also, the stressed bending of C = O were detected around 1,570 cm^{-1} and 450-525 cm^{-1}. This stressed swing is directly related to TiO_2 molecules.

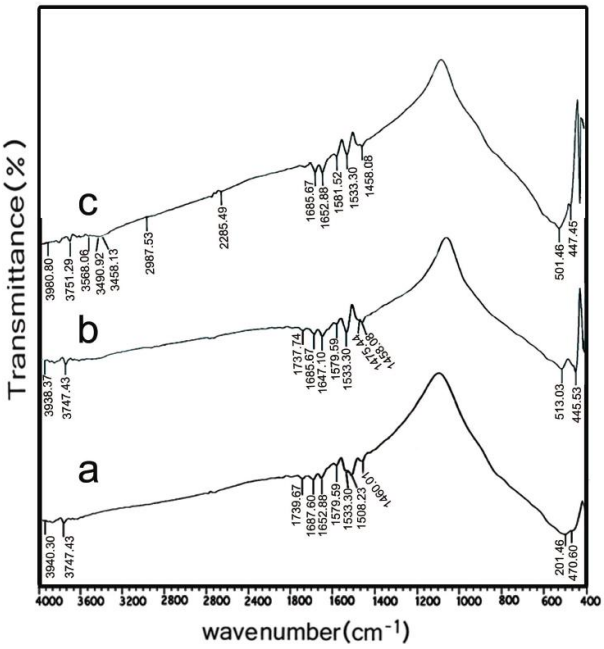

Fig. 3. FTIR spectra of: (a) 0.1 M, (b) 0.3 M and (c) 1M TiO_2 nanoparticles.

The bactericidal activity of the TiO_2 nanoparticles were investigated against *Eschericchia coli* PTCC 1395 bacteria, as presented in Fig. 4. It is seen that the number of viable bacteria reduced in the presence of TiO_2 nanoparticles. The results showed that TiO_2 nanoparticle has significant antibacterial effect on *Escherichia coli* PTCC 1395 at concentration of 1mg/mL. By increasing of molarity from 0.1 to 1M is decreasing the viable cell concentration of *E. coli* from 88.89 % to 8.33 % after 3 hours. Since the experiments have been carried out in unique conditions (different photocatalysts, pH, temperature, light source, microbial strains), a comparison of data obtained by various research groups seems to be problematic. Desai and Kowshik synthesized polycrystalline TiO_2 by sol-gel technique [38]. They studied the killing curves for *Escherichia coli*, *Pseudomonas aeruginosa*, *Klebsiella pneumoniae* and *Staphylococcus aureus*. From an initial count of 10^5 CFU mL^{-1}, a 2 log reduction (99 %) in viable count could be obtained after 20 min of exposure, in the case of *Klebsiella pneumoniae* and *Pseudomonas aeruginosa*, whereas for *Staphylococcus aureus*, a 1 log reduction (90 %) was obtained after exposure for the same interval of time. At the end of 40 min, a 5 log reduction (99.999 %) was obtained for *Klebsiella pneumoniae*, *Pseudomonas aeruginosa* and *Staphylococcus aureus*. The extent of the TiO_2 photocatalytic effect is inversely proportional to the thickness and complexity of the microbe cell wall. The antibacterial activity of TiO_2 is related to ROS production, especially hydroxyl free radicals and peroxide formed under UV-B irradiation *via* oxidative and reductive pathways, respectively.

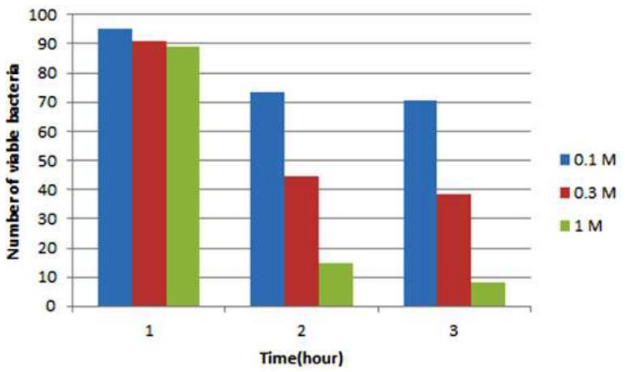

Fig. 4. Survival ratio of Escherichia coli PTCC 1533 in the presence of TiO_2 nano powder of various molarity.

On the other hand, it was observed that *Escherichia coli* exhibited minimal susceptibility to 0.1 M of TiO_2. In all these experiments we observed that the efficiency of the process was reduced when the bacterial suspensions were not stirred continuously on a magnetic stirrer. To evaluate this, we stirred manually bacterial suspension + TiO_2, once every 2 min. Thus, the bactericidal action of TiO_2 was dependent on the amount of dissolved molecular oxygen and proper cell-TiO_2 contact (both of them are increased during stirring). It has been reported earlier that, since TiO_2 photoreacts with oxygen present in H_2O, more dissolved oxygen produce more $^{\bullet}OH$ radicals by scavenging the conduction band electrons and reducing the rate of EHP recombination. Thus, the lack of sufficient oxygen reduces the rate of reaction [13]. In addition, free movement of the nanoparticles in suspension form facilitates the proper contact with microbes and accelerates the translocation of nanoparticles through the bacterial cell membrane [39]. A closer analysis of the survival curves of the microorganisms revealed that the inactivation had occurred in two distinct phases, the microorganisms being not much affected in the first 10 min. This could be due to the presence of $^{\bullet}OH$ radicals scavengers in water that can react with $^{\bullet}OH$ radicals generated by TiO_2 and reduce the efficiency of the inactivation process [40]. Galvez et al have studied the mechanism of bactericidal activity of TiO_2 [41]. They found that oxidative damage first takes place on the cell wall when the TiO_2 makes contact with the cell. Even after the first contact of TiO_2 with the cells, they are still viable, however, as photocatalytic action progresses the cell permeability increases so that much higher levels of TiO_2 particles get into cells and cause photo oxidation of intracellular components thereby accelerating cell death. This further explains the initial delay in the bactericidal activity of TiO_2 nanoparticles. Our results of the antimicrobial study complies with the earlier findings by Matsunaga *et al.* [42] and other researchers observing that irradiated TiO_2 exhibits bactericidal activity [41] and that the efficacy of this disinfection process is proportionally correlated with the TiO_2 dose and the exposure time. Bondoux and colleagues stated that the sol-gel method of TiO_2 synthesis, as compared to other methods, is easier and cheaper [43]. Robertson et al [44] using Degussa P25 material at a concentration of 1 mg mL^{-1}, obtained a 3 log reduction of *Pseudomonas aeruginosa* during 2 h, which is comparable to the results obtained in this work; however, they used a 480 W lamp with a 330 to 450 nm wavelength range, which had a bactericidal activity confirmed in the controls when the test was performed in the absence of Degussa P25, obtained for exposing the cells to UV light; higher percentages of inhibition were reached.

4. Conclusion

Titanium dioxide nanopowders were synthesized by the facile sol-gel technique. The bactericidal properties of the synthesized compound were confirmed in an aqueous solution. It was found that the prepared nanoparticles have a significant antibacterial effect on *Escherichia coli* PTCC 1395 at concentration of 1mg/mL. The efficacy of this activity was increased with the molarity of TiO_2 solution. The results verify previous reports of the privileged physical and chemical properties of synthesized TiO_2 powder (namely, strong oxidizing and photocatalytic activity) that render it as an effective bactericidal material.

Acknowledgements

This work was supported by Islamic Azad University of Lahijan Branch and authors would like to thank gratefully the Research Council for financial support of this work.

References

[1] A. A. Ashkarran, J. Theor. Appl. Phys. **4**, 1 (2011).
[2] M. S. Hoffmann, T. Martin, W. Choi, D. W. Bahnemann, Chem. Rev. **95**, 69 (1995).
[3] D. F. Ollis, Environ. Sci. Technol. **19**, 480 (1985).
[4] J. C. Yu, J. G. Yu, W. K. Ho, L. Z. Zhang, Chem. Commun. 1942 (2001).
[5] M. A. Fox, M. T. Duby, Chem. Rev. **93**, 341 (1993).
[6] G. A. Somorjai, Chem. Rev. **96**, 1223 (1996).
[7] J. C. Yu, W. Ho, J. Lin, H. Yip, P. K. Wong, Environ. Sci. Technol. **37**, 2296 (2003).
[8] J. S. Hur, Y. Koh, Biotechnol. Lett. **24**, 23 (2002).
[9] K. Sunada, T. Watanabe, K. Hashimota, J. Photochem. Photobiol. A, chemistry. **156**, 227 (2003).
[10] P. C. Maness, S. Smolinski, D. M. Blake, Z. Huang, E. J. Wolfrum, W. A. Jacoby, Appl. Environ. Microbiol. **65**, 4094 (1999).
[11] D. Gumy, C. Morais, P. Bowen, C. Pulgarin, S. Giraldo, R. Hajdu, J. Kiwi, Appl. Catal. B, **63**, 76

(2006).
[12] D. Blake, P. C. Maness, Z. Huang, E. Wolfrum, J. Huang, W. A. Jacoby, Separ. Purif. Method. **28**, 1 (1999).
[13] M. Cho, H. Chung, W. Choi, J. Yoon, J. Water. Res. **38**, 1069 (2004).
[14] K. E. Hammel, A. N. Kpich, K.A. Jensen, Z. C. Ryan, Enzym. Microb. Tech. **30**, 445 (2002).
[15] Z. Huang, P. C. Maness, D. M. Blake, E. J. Wolfrum, S. L. Smolinski, W. A. Jacoby, J. Photochem. Photobiol. A, Chem. **130**, 163 (1999).
[16] J. C. Ireland, P. Klostermann, E. W. Rice, R. M. Clark Appl. Environ. Microbiol. **59**, 1668 (1993).
[17] K. P. Kuhn, I. F. Chaberny, K. Masholder, M. Stickler, V. W. Benz, H. G. Sonntag, L. Erdinger, Chemosphere. **53**, 71 (2003).
[18] A. Makowski, W. Wardas, Curr. Top. in Bioph. **25**, 19 (2001).
[19] T. Saito, T. Iwase, T. Morioka, J. Photochem. Photobiol. B, **14**, 369 (1992).
[20] J. C. Sjogren, R. A. Sierka, Appl. Environ. Microbiol. **60**, 344 (1994).
[21] C. Srinivasan, N. Somasundaram, Current. Science. **85**, 1431 (2003).
[22] R. J. Watts, S. Kong, M. P. Orr, G. C. Miller, B. E. Henry, J. Water. Res. **29**, 95 (1995).
[23] M. Bekbolet, C. V. Araz, Chemosphere. **32**, 959 (1996).
[24] N. Daneshvar, A. Niaei, S. Akbari, S. Aber, N. Kazemian, J. Global. NEST. **9**, 132 (2007).
[25] C. Maneerat, Y. Hayata, Int. J. Food Microbiol. **107**, 99 (2006).
[26] D. Mitoraj, A. Janczyk, M. Strus, H. Kisch, G. Stochel, P. B. Heczko, W. Macyk, J. Photochem. Photobiol. Sci. **6**, 642 (2007).
[27] A. R. Rahmani, M. R. Samarghandi, M. T. Samadi, F. Nazemi, J. Res. Health. Sci. **9**, 1 (2009).
[28] A. G. Rincon, C. Pulgarin, Appl. Catal. B, **4**, 99 (2004).
[29] D. D. Sun, J. H. Tay, K. M. Tan, J. Water. Res. **37**, 3452 (2003).
[30] R. Van Grieken, J. Maguran, C. Pablos, L. Furones, A. Lypez, Appl. Catal. B, Environ. **100**, 212 (2010).
[31] S. Rana, M. Brown, A. Dutta, A. Bhaumik, C. Mukhopadhyay, Tetrahedron Lett. **54**, 1371 (2013).
[32] C. Wei, W. Y. Lin, Z. Zainal, N. E. Williams, K. Zhu, A. P. Kruzic, R. L. Smith, K. Rajeshwar, Environ. Sci. Technol. **28**, 934 (1994).
[33] J. C. Yu, H. Y. Tang, J. Yu, H. C. Chan, L. Zhang, Y. Xie, H. Wang, S. P. Wong, J. Photochem. Photobiol. A, **153**, 211 (2002).
[34] A. R. Khataee, H. Aleboyeh, A. Aleboyeh, J. Exp. Nanosci. **4** (2), 121 (2009).
[35] S. Amemiya, Three Bond Tech. news. **62**, 1 (2004).
[36] K. Hirakawa, M. Mori, M. Yoshida, S. Oikawa, S. Kawanishi, Free Radic. Res. **38**, 439 (2004).
[37] S. Lee, N. M. Otaki, S. Ohgaki, J. Water. Sci. Technol. **35**, 101 (1997).
[38] S. Vilas Desai, M. Kowshik, Res. J. Microbiol. **4**, 97 (2009).
[39] D. N. Williams, S. H. Ehrman, T. R. P. Holoman, J. Nanobiotechnol. **4**, 1 (2006).
[40] T. A. Egerton, A. M. Samia Kosa, P. A. Christensen, J. Phys. Chem. **8**, 398 (2005).
[41] J. B. Galvez, P. F. Ibanez, M. R. Sixto, J. Solar. Energy. Eng, **129**, 12 (2007).
[42] T. Matsunaga, R. Tomoda, T. Nakajima, H. Wake, FEMS Microbiol. Lett. **29**, 211 (1985).
[43] C. Bondoux, P. Prene, P. Belleville, F. Guillet, S. Labert, B. Minot, R. Jerisian, J. Euro. Ceram. Soc. **25**, 2795 (2005).
[44] J. M. C. Robertson, P. K. J. Robertson, L. A. Lawton, J. Photoch. Photobio. A, **175**, 51 (2005).

*Corresponding author: ali_abdolahzadeh@liau.ac.ir